Composites: Part A xxx (2016) xxx–xxx

Contents lists available at ScienceDirect

Composites: Part A

journal homepage: www.elsevier.com/locate/compositesa

Enhanced microwave absorption properties of flake-shaped FePCB metallic glass/graphene composites

Dan Chuai [a], Xiaofang Liu [a,*], Ronghai Yu [a,*], Jinrui Ye [b], Youqiang Shi [c]

[a] School of Materials Science and Engineering, Beihang University, Beijing 100191, China
[b] Association for Science and Technology of Beihang University, Beijing 100191, China
[c] AVIC Beijing Institute of Aeronautical Materials, Beijing 100195, China

ARTICLE INFO

Article history:
Available online xxxx

Keywords:
A. Graphene
A. Hybrid
B. Electrical properties
B. Magnetic properties

ABSTRACT

A novel kind of composite absorber, i.e. FePCB/graphene composite, with excellent microwave absorption properties was successfully fabricated by a simple and scalable ball milling method. After being milled, the FePCB particles displayed flaky morphology with large aspect ratio. The complex permittivity and permeability of the flaky FePCB distinctly increased compared with those before milling. Furthermore, with the introduction of graphene, the flaky FePCB/graphene composite exhibited excellent microwave absorption performance with strong absorption and wide absorption band. In particular, for FePCB/graphene composite with an absorber thickness of 2 mm, the reflection loss (RL) reached a minimum of −45.3 dB at 12.6 GHz and the effective absorption bandwidth (RL < −10 dB) covered 5.4 GHz. The enhanced microwave absorption performance of the FePCB/graphene composite was attributed to the high magnetic loss and improved impedance matching which were closely related to the flake-shaped FePCB particles and the introduction of graphene sheets.

1. Introduction

With the high demands for the reduction of the electromagnetic (EM) radiation and improvement of anti-electromagnetic interference, microwave absorbing materials with the capability of absorbing EM signal are widely applied in industry and military [1–3]. Among the candidates for EM wave absorbers, Fe-based soft magnetic metals/alloys such as Fe [4], FeNi [5], FeCo [6] and FeSiAl [7] have attracted considerable interest because of their outstanding soft magnetic properties and potential applications in high-frequency devices and micro-transductions which require high saturation magnetization, large susceptibility and high Curie temperature. However, the metal/alloy magnetic absorbers often suffer from narrow absorbing frequency bandwidth, large layer thickness, EM mismatch, easy oxidation and corrosion, which hinder their applications in absorbing EM wave.

Fe–P–C metallic glass is an important soft magnetic material and has been widely used as the key parts in many magnetic devices due to its high saturation magnetization, high permeability, good mechanical property and low cost [10]. These advantages also endow the Fe–P–C metallic glass an attractive microwave absorbing material in practical applications. Moreover, the amorphous structure and unique composition of the Fe–P–C metallic glass causes the decrease of conductivity relative to the Fe-based crystalline alloy, which is favorable to reducing the impedance mismatch. Nevertheless, to the best of our knowledge, the microwave absorbing properties of the Fe–P–C based metallic glass have not been reported yet.

Recently, the synthesis of magnetic–dielectric composite absorbers, which can take advantages of both a unique permittivity and strong magnetic properties, have received increasing attention [8,9]. Compared with other dielectric additives, carbon-based materials including carbon nanotubes [14], carbon black [15], graphite [16] and graphene [10–13] possess exceptional advantages of low density, high thermal stability and high chemical stability. Until now, many carbonaceous material-alloy composites have been prepared and exhibited strong EM wave absorbing property. For example, Liu et al. prepared (Fe, Ni)/C nanocapsules using arc discharge technique and obtained an optimal reflection loss of −32 dB with 2 mm thickness layer [9]. Chen et al. deposited Fe nanoparticles on graphene nanosheets, and this material exhibited good microwave absorbing properties with the minimum reflection loss of −31.5 dB at 14.2 GHz with a thickness of 2.5 mm

* Corresponding authors. Tel.: +86 10 82317101.
E-mail addresses: liux05@buaa.edu.cn (X. Liu), rhyu@buaa.edu.cn (R. Yu).

http://dx.doi.org/10.1016/j.compositesa.2016.02.010
1359-835X/

[14]. Bateer et al. found that the Fe_3C/graphitic carbon/paraffin composite containing 70 wt.% Fe_3C/graphitic carbon displayed good microwave absorption abilities with an optimal reflection loss of −26 dB for the 2 mm thickness layer [1]. All of these encourage us to develop a novel FePCB–carbonaceous material composite absorber. The addition of carbonaceous material may play important roles in tuning the permittivity and improving the impedance matching, which benefit the enhancement of microwave absorption performance.

In this work, FePCB alloy powder with a potato-like shape mixed with light-weight graphene sheets, was ball-milled to achieve a flake-shaped FePCB–graphene composite absorber. The obtained FePCB flakes have higher permeability in gigahertz frequency due to their large aspect ratio, and exhibited strong magnetic loss. Simultaneously, graphene sheets are used as a light-weight dielectric addictive to improve the impedance matching of the FePCB metallic glass. Relative to other carbonaceous materials, graphene sheets have larger surface areas, and their flexible laminated structure benefits the close contact with FePCB particles during ball milling process. The prepared FePCB/graphene composite displayed an excellent microwave absorption performance with strong absorption, wide absorption bandwidth and a thin layer thickness.

2. Experimental method

2.1. Preparation of FePCB/graphene composite

A micrometer-sized $Fe_{0.2}P_{0.05}C_{0.45}B_{0.3}$ alloy powder fabricated by a water spray method was used as the starting material. The shape of the raw powder was potato-like and the size was in the range of 2–32 μm. The graphene sheets with diameter and thickness of 5–10 μm and 3–10 nm, respectively, were purchased from Nanjing XFNANO Materials Tech (Nanjing, China). The conductivity of the graphene was 500–1000 S/cm. The SEM images of the graphene sheets are given in the supporting information (Fig. S1). The FePCB/graphene composite was obtained by ball milling the mixed powders of FePCB and graphene for 4 h. The mass fraction of graphene to FePCB was 4 wt.%. The ball-to-powder ratio was set at 40:1 by weight with the rotation speed of 178 rpm. Certain content of anhydrous ethanol was added into the powder as the process control agent. After ball milling, the powders were collected and dried in oven at 60 °C.

2.2. Characterization

The crystal structure was determined by X-ray diffraction (XRD, Rigaku, model D/max-2500 system at 40 kV and 100 mA of Cu Ka). The morphology and the size of the powder were characterized by scanning electron microscopy (SEM, JEOL JSM-7500F). Raman spectra were obtained using an in Via Laser Raman spectrometer (LabRAm HR Evolution). The magnetic properties were measured by a vibrating sample magnetometer (VSM, Lake Shore 7307) at room temperature. The measurements of the room-temperature conductivity were carried out on four-point probes resistivity measurement system (RTS-8).

For electromagnetic (EM) parameter measurements, the powder samples with weight ratio of 60 wt.% were uniformly mixed with paraffin. The as-prepared mixture was then pressed into toroidal-shaped specimens with outer diameter of 7.00 mm and inner diameter of 3.04 mm. EM parameters were measured by a vector network analyzer (Agilent Technologies, PNA-L, N520C) in the range of 2–18 GHz.

3. Results and discussion

XRD measurements were used to investigate the crystalline structure of the samples. As shown in Fig. 1, the XRD pattern of the raw FePCB powder displays a broad diffraction hump at 45° and three sharp diffraction peaks at 43°, 50°, 74°, respectively. It reveals that the raw FePCB alloy consists of both nanocrystalline and amorphous phases. The broad hump corresponds to the bcc structured α-Fe with metallic glassy feature, while the three sharp peaks can be indexed to Fe_3P phase. After ball milling, the three sharp peaks become indistinct indicating the disappearance or significant decrease of Fe_3P phase during the milling process. As for FePCB/graphene composite, the XRD curve exhibits strong diffraction peaks of α-Fe phase along with a weak peak at 25.6°. The new peak could be attributed to the disordered (002) stacking layers of graphene [15].

Fig. 2 shows the morphology of the raw FePCB, as-milled FePCB and FePCB/graphene composite. The raw FePCB alloy exhibits potato-like shape with wide distribution of particle size from 2 to 32 μm. After ball milling, the FePCB particles deformed into flake shape with an increase of plane size and a decrease of thickness (Fig. 2b). Hence, the aspect ratio of the as-milled particles (plane size/thickness) considerably increases relative to the raw powder. Since the large aspect ratio of the particle could suppress eddy currents in high-frequency electromagnetic field and limit the magnetic moments to the plane of the particles thereby increasing permeability, such shape deformation would benefit the microwave absorption capability of the FePCB alloy. As presented in Fig. 2(c), the stacking structure of the graphene sheets did not change during the ball milling process, and the stacking layers of graphene were uniformly mixed with the FePCB alloy flakes. The compositions of the three samples were determined by EDS. As illustrated in Fig. 2(d)–(f), the elemental ratio of the as-milled FePCB alloy is consistent with that of the raw material. The C ratio of the FePCB/graphene composite obviously increases due to the addition of graphene.

Raman spectroscopy is a powerful tool to distinguish ordered and disordered crystal structures of carbon [16]. Fig. 3 presents the Raman spectra of the graphene and FePCB/graphene composite. Two characteristic peaks at ~1340 and 1600 cm^{-1} appear in graphene spectrum, which correspond to the D band and G band, respectively [17]. The D band is a first-order zone boundary phonon mode associated with defects in the graphene or graphene edge, while the G band is a radial C–C stretching mode of sp^2 bonded carbon [18]. In general, the intensity ratio of D band to G

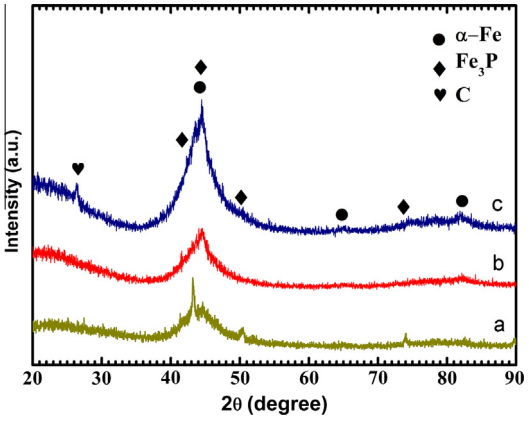

Fig. 1. XRD patterns of raw FePCB (a), as-milled FePCB (b) and FePCB/graphene composite (c). (For interpretation of the references to colour in this figure legend, the reader is referred to the web version of this article.)

Please cite this article in press as: Chuai D et al. Enhanced microwave absorption properties of flake-shaped FePCB metallic glass/graphene composites. Composites: Part A (2016), http://dx.doi.org/10.1016/j.compositesa.2016.02.010

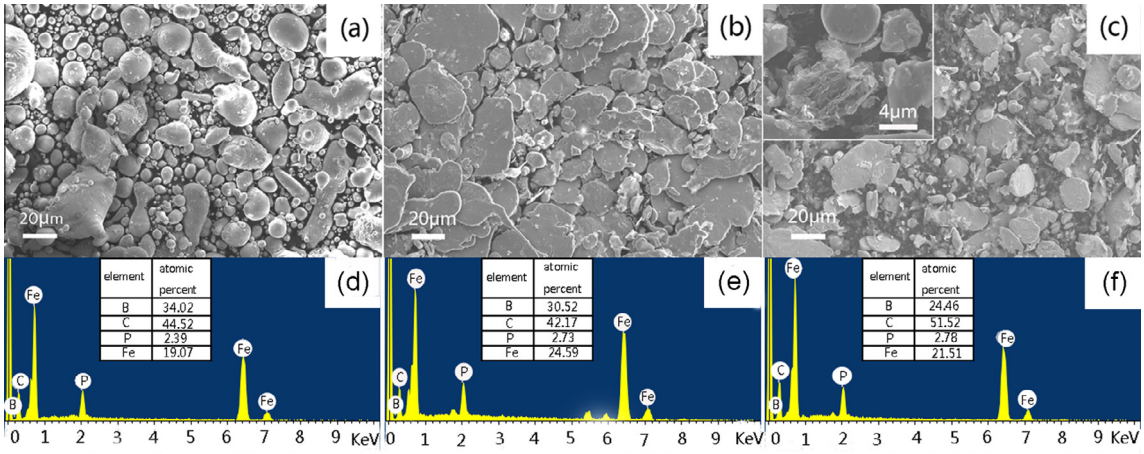

Fig. 2. SEM images and EDS results of raw FePCB (a) and (d), as-milled FePCB (b) and (e), and FePCB/graphene composite (c) and (f). The inset in (c) shows a magnified image of the graphene sheets in FePCB/graphene composite. (For interpretation of the references to colour in this figure legend, the reader is referred to the web version of this article.)

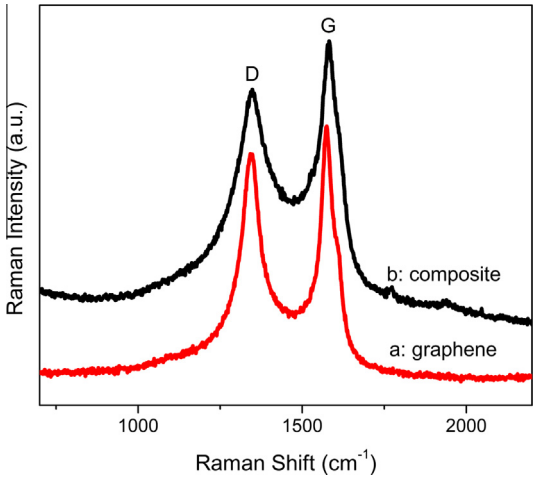

Fig. 3. Raman spectra of graphene and FePCB/graphene composite. (For interpretation of the references to colour in this figure legend, the reader is referred to the web version of this article.)

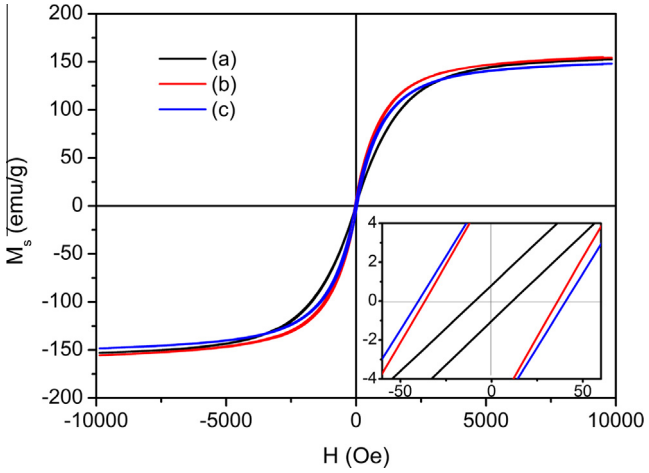

Fig. 4. Room-temperature magnetization curves of FePCB (a), as-milled FePCB (b), and FePCB/graphene composite (c). (For interpretation of the references to colour in this figure legend, the reader is referred to the web version of this article.)

band (I_D/I_G) as well as the intensity and shape of the D and G peaks are correlated with the degree of order of carbon structure. The high I_D/I_G value (~0.9) of the pure graphene (curve a) indicates the presence of large number of defects in graphene sheets. Compared with pure graphene, the D and G peaks of the FePCB/graphene composite become broader and weaker, suggesting a further reduced degree of order of carbon structure. The high degree of disorder and the presence of large amount of defects lead to the low conductivity of graphene sheets (10^3 S/cm)

The field dependences of magnetizations for the FePCB, as-milled FePCB and FePCB/graphene composite were measured by VSM at room temperature, as shown in Fig. 4. Details of saturation magnetization (M_s) and coercivity (H_c) are listed in Table 1. The raw FePCB alloy with M_s value of 152.71 emu/g displays a typical soft magnetic characteristic with rather small H_c value. It is clear that ball milling largely increased the H_c of the FePCB alloy which may be correlated to the decreased grain size, increased internal strain as well as the increased defect density that inducing a higher resistance to the magnetization due to the pinning effect [19]. Compared with the raw and as-milled FePCB alloys, the FePCB/graphene composite shows a reduced M_s value owing to the introduction of nonmagnetic graphene.

Table 1
Magnetic properties of raw FePCB, as-milled FePCB and FePCB/graphene composite.

	M_s (emu/g)	H_c (Oe)
FePCB	152.71	10.31
As-milled FePCB	155.31	36.45
FePCB/graphene composite	148.16	40.41

The microwave absorption properties of the raw FePCB, as-milled FePCB and FePCB/graphene composite were investigated in terms of the relative complex permittivity (ε_r) and relative complex permeability (μ_r). The reflection loss (RL) values of the samples were calculated by the following equations at a given frequency and layer thickness according to the transmit line theory [20]:

$$\mathrm{RL(dB)} = 20\log\left|\frac{Z_{in}-Z_0}{Z_{in}+Z_0}\right| \quad (1)$$

$$Z_{in} = \sqrt{\frac{\mu_r}{\varepsilon_r}}\tanh\left(j\frac{2\pi fd}{c}\sqrt{\mu_r\varepsilon_r}\right) \quad (2)$$

Please cite this article in press as: Chuai D et al. Enhanced microwave absorption properties of flake-shaped FePCB metallic glass/graphene composites. Composites: Part A (2016), http://dx.doi.org/10.1016/j.compositesa.2016.02.010

where Z_0 is the impedance of free space, Z_{in} is the input impedance of the absorber, f is the EM wave frequency, d is the thickness of the absorber layer, c is the velocity of electromagnetic wave in vacuum.

High-performance microwave absorbing material is expected to exhibit low RL with thin absorber thickness and wide absorption range. Figs. 5 and S2 show the calculated RLs of the FePCB, as-milled FePCB and FePCB/graphene composite with different thickness. It is found that the thickness of the absorber has a large influence on the microwave absorbing properties. The minimum RL peak gradually shifts toward lower frequency with the increase of absorber thickness, which follows the formula [21]

$$d_m = \frac{\lambda_m}{4} = \frac{c}{4f_m\sqrt{\varepsilon_r\mu_r}} \quad (3)$$

where f_m and d_m are the matching frequency with the minimum RL and the sample thickness, respectively. It is seen from Fig. 5 that the shape deformation of the FePCB alloy and the introduction of graphene evidently improve the microwave absorbing property. The minimum RL value of the raw FePCB alloy is −23.8 dB at 9.2 GHz with a thickness of 3 mm (Fig. 5(a)). After ball milling, the minimum RL value decreases to −39.6 dB at 5.0 GHz with a thickness of 3.5 mm (Fig. 5(b)). As to the FePCB/graphene composite (Fig. 5(c)), it is surprising that the minimum RL value reaches −45.3 dB at 12.6 GHz with a thickness of only 2 mm. Simultaneously, the bandwidth of RL value less than −10 dB covers 5.4 GHz (from 10.1 to 15.5 GHz). Compared with other Fe-based absorbers, the microwave absorption of the FePCB/graphene composite with a thickness of 2 mm is superior to those in the previous reports: Fe/amorphous SnO_2 core–shell structured nanocapsules (−39.2 dB at 16.8 GHz, 2 mm) [22], $Fe_{0.65}Co_{0.35}/Fe_3O_4$ composite (−41.4 dB at 2.02 GHz, 6.0 mm) [23], Fe–Cr–Ni flaky alloy (−27 dB at 5.6 GHz, 2.3 mm) [24], and surface-oxidized FeSiAl flaky alloys (−39.67 dB

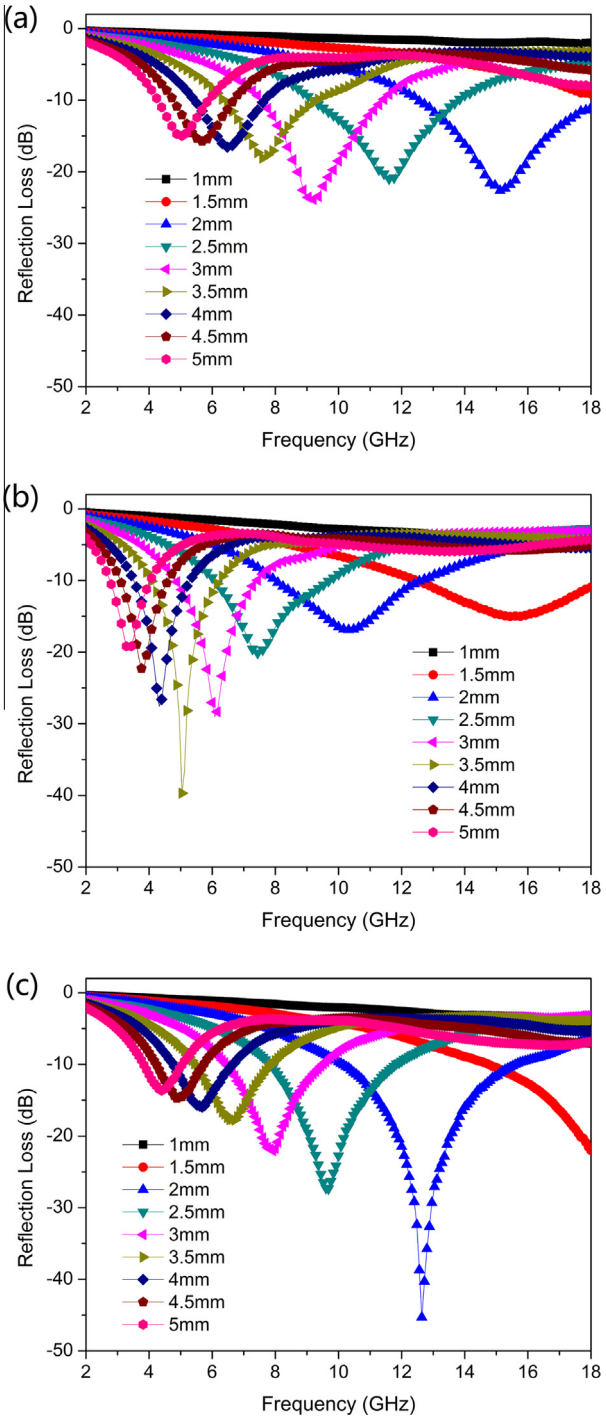

Fig. 5. Reflection losses of raw FePCB (a), as-milled FePCB (b), and FePCB/graphene composite. (For interpretation of the references to colour in this figure legend, the reader is referred to the web version of this article.)

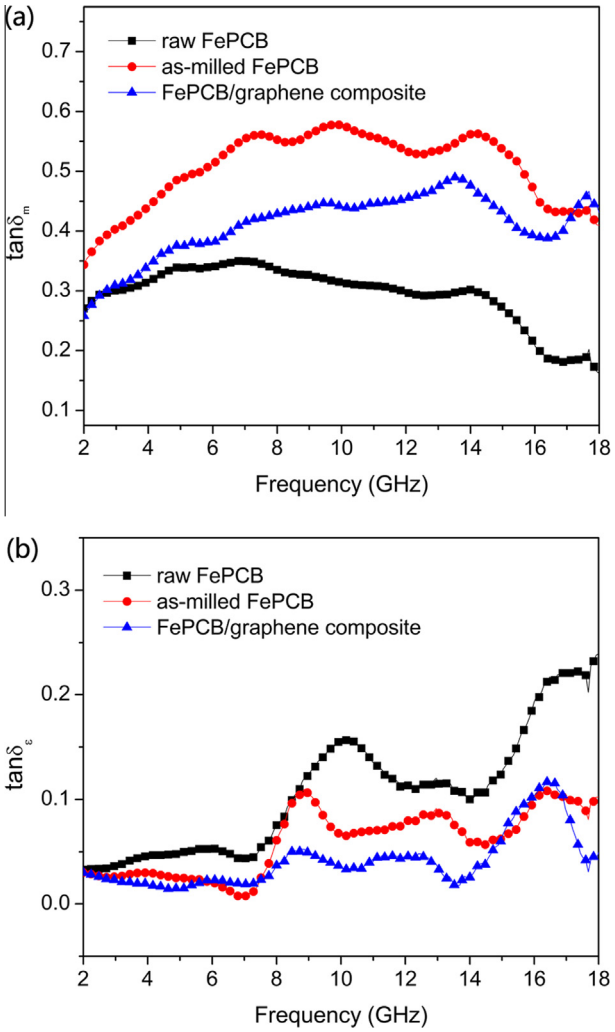

Fig. 6. Magnetic loss tangents (a) and dielectric loss tangents (b) of raw FePCB, as-milled FePCB and FePCB/graphene composite. (For interpretation of the references to colour in this figure legend, the reader is referred to the web version of this article.)

Please cite this article in press as: Chuai D et al. Enhanced microwave absorption properties of flake-shaped FePCB metallic glass/graphene composites. Composites: Part A (2016), http://dx.doi.org/10.1016/j.compositesa.2016.02.010

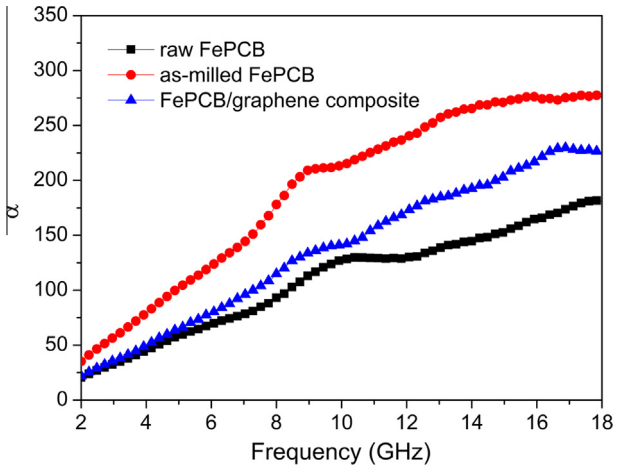

Fig. 7. Attenuation constants of raw FePCB, as-milled FePCB and FePCB/graphene composite as a function of frequency. (For interpretation of the references to colour in this figure legend, the reader is referred to the web version of this article.)

at 1.40 GHz, 4 mm) [7]. Therefore, the FePCB/graphene composite with the advantages of strong absorption and small thickness can be considered as a promising candidate for high-performance microwave absorber in practical applications.

To clarify the possible microwave absorption mechanism, Fig. 6 shows the magnetic tangent loss ($\tan\delta_m = \mu''/\mu'$) and dielectric tangent loss ($\tan\delta_e = \varepsilon''/\varepsilon'$) of the three samples, which were calculated based on the measured complex permeabilities and complex permittivities. Generally, the loss tangent ($\tan\delta$) represents the loss properties of the incident EM wave in an absorber. As shown in Fig. 6(a) and (b), the $\tan\delta_m$ values of the raw FePCB, as-milled FePCB and FePCB/graphene composite are in the range of 0.16–0.35, 0.41–0.58 and 0.26–0.49, respectively, while the $\tan\delta_e$ values are all below 0.2. The much larger values of $\tan\delta_m$ suggests that the magnetic loss dominates the attenuation of EM energy over the whole frequency range. It is widely known that excellent microwave absorbing performance depends on two critical factors, i.e. strong EM wave attenuation and good impedance matching. The attenuation constant (α), which reflects the EM wave attenuation ability of an absorber, is estimated from the following equation [25]:

$$\alpha = \frac{\pi f}{c}\sqrt{\mu'\varepsilon'}\sqrt{2(\tan\delta_\varepsilon \tan\delta_m - 1 + \sqrt{1+\tan^2\delta_\varepsilon + \tan^2\delta_m + \tan^2\delta_\varepsilon\delta_m})} \quad (4)$$

From Fig. 7, it is found that the as-milled FePCB alloy displays the largest attenuation constant, which suggests that this material can achieve the maximum attenuation of the entered EM wave. Nevertheless, the previous reflection loss calculation demonstrated that the microwave absorption property of the FePCB/graphene composite is superior to the as-milled FePCB alloy. Therefore, the impedance matching which is another critical factor for determining the absorbing property should be taken into account by analyzing the complex permittivities and complex permeabilities of the samples.

Fig. 8(a) and (b) shows the real and imaginary parts of the complex permeabilities of the raw FePCB, as-milled FePCB and FePCB/graphene composite. The μ' values of the raw FePCB, as-milled FePCB and FePCB/graphene composite begin from 1.49, 1.87 and

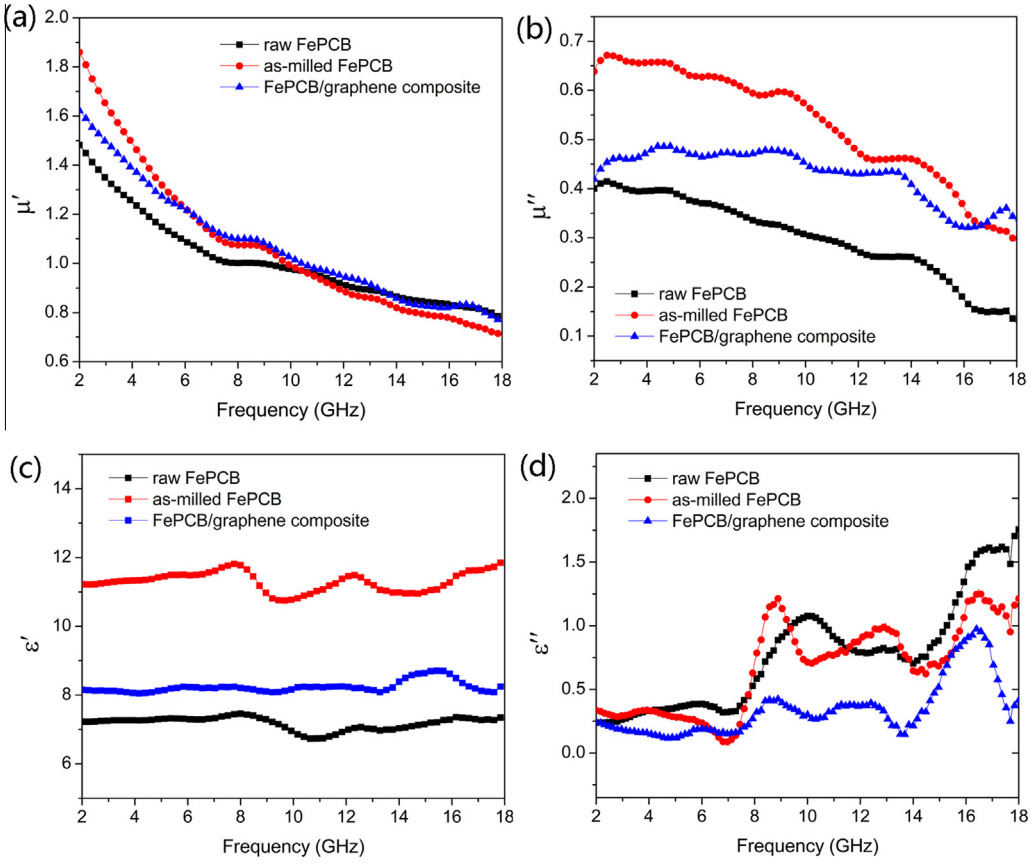

Fig. 8. Relative complex permeabilities and complex permittivities of raw FePCB, as-milled FePCB and FePCB/graphene composite. (For interpretation of the references to colour in this figure legend, the reader is referred to the web version of this article.)

Please cite this article in press as: Chuai D et al. Enhanced microwave absorption properties of flake-shaped FePCB metallic glass/graphene composites. Composites: Part A (2016), http://dx.doi.org/10.1016/j.compositesa.2016.02.010

1.63, respectively (at 2 GHz), and show a sharp decrease trend with increasing frequency. The μ'' values of the raw FePCB and as-milled FePCB alloys gradually decrease with frequency whereas the μ'' values of the FePCB/graphene composite slightly fluctuate in 2–14 GHz followed by an obvious decrease in 14–18 GHz. The maximum μ'' values of the raw FePCB, as-milled FePCB and FePCB/graphene composite are 0.41, 0.67 and 0.48, respectively. Compared with raw FePCB alloy with potato-like shape, the increase in permeabilities of the as-milled FePCB and FePCB/graphene composite can be ascribed to the large aspect ratio of the flaky FePCB particles. On one hand, the exchange coupling reaction of the magnetic moment between particles can be enhanced with the increase of surface area; on the other hand, the eddy current loss, which may decrease the permeability, is reduced in flaky particles [26]. Additionally, the permeability strongly depends on the saturated magnetization (M_s) of materials ($(\mu_0 - 1)f_0 = M_s/3\pi$) [27]. The introduction of nonmagnetic graphene reduces the M_s value (shown in Fig. 4), thus leading to the drop of permeability of the FePCB/graphene composite.

As presented in Fig. 8(c) and (d), the ε' values of the raw FePCB alloy are in the range of 6.63–7.52, and the ε'' values fluctuate from 0.21 to 1.77. After ball milling, the ε' values of the FePCB flakes considerably increase to 10.64–11.88 while the ε'' values are almost in the same level. The larger ε' values suggest the enhanced polarizations. In FePCB/paraffin sample, the interfacial polarizations from the interfaces between FePCB particles and paraffin matrix is the main origin of polarizations. Relative to the potato-like FePCB particles, the flaky particles with higher aspect ratio have larger specific surface area, which then contributes to an enhanced overall interfacial polarization. As to the FePCB/graphene composite, the average ε' value is 8.31 and the ε'' values vary from 0.15 to 1.00. The decrease in permittivity after the incorporation of graphene is possibly caused by the increase of resistivity according to the free electron theory [28]. The resistivity of the as-milled FePCB alloy was measured by four-point probe method and the value is $4 \times 10^{-4}\ \Omega$ cm. However, as previously indicated in Raman spectra, the graphene we used contains a large number of defects, thus inducing a relatively lower conductivity of $10^{-3}\ \Omega$ cm. Hence the FePCB/graphene composite possesses the decreased permittivity by mixing with graphene.

To obtain low reflection, good impedance matching has to be fulfilled to allow EM wave entering into the absorbing materials to the greatest extent. As stated above, the huge imbalance between ε' and μ' of the as-milled FePCB alloy results in the poor impedance matching. After combining with graphene, the considerable drop of the ε' of the FePCB/graphene composite effectively improves the impedance matching and thus benefits the microwave absorbing property. Besides, the planar shape of FePCB particles and graphene sheets are beneficial to the multi reflections and scattering of EM wave, which could be a minor reason for the EM wave attenuation [10]. When the FePCB alloy was replaced by the equal weight of graphene, the probability of the multi reflections and scattering would increase, thus further enhancing the absorbing ability. As a result, it is concluded that the excellent microwave absorption property of the FePCB/graphene composite can be attributed to the following factors: (1) the improved the impedance matching character; (2) the large magnetic loss; (3) the enhanced multi reflections and scattering.

4. Conclusions

A novel FePCB/graphene composite with enhanced microwave absorption properties were successfully fabricated by a simple ball milling method. After being milled, the FePCB particles displayed flaky shape with large aspect ratio. The shape transformation of the FePCB particles resulted in the increase of magnetic loss, while the introduction of graphene improved the impedance matching of the composite. The FePCB/graphene composite exhibited excellent microwave absorption performance in gigahertz frequency. The minimum RL reached −45.3 dB at 12.6 GHz with a layer thickness of 2 mm, and the absorption bandwidth with the RL values below −10 dB was about 5.4 GHz in the range of 10.1 to 15.5 GHz. These results indicated that the flake-shaped FePCB/graphene composite could serve as a potential EM wave absorber in gigahertz frequency range.

Acknowledgements

This work was supported by Beijing Municipal Science and Technology Project (No. D14110300240000) and the National Natural Science Foundation of China (Nos. 51102006 and 51472012).

Appendix A. Supplementary material

Supplementary data associated with this article can be found, in the online version, at http://dx.doi.org/10.1016/j.compositesa.2016.02.010.

References

[1] Bateer B, Wang L, Zhao L, Yu P, Tian C, Pan K, et al. A novel Fe_3C/graphitic carbon composite with electromagnetic wave absorption properties in the C-band. RSC Adv 2015;5(74):60135–40.
[2] Wang T, Li Y, Wang L, Liu C, Geng S, Jia X, et al. Synthesis of graphene/α-Fe_2O_3 composites with excellent electromagnetic wave absorption properties. RSC Adv 2015;5(74):60114–20.
[3] Zhang L, Shi C, Rhee KY, Zhao N. Properties of $Co_{0.5}Ni_{0.5}Fe_2O_4$/carbon nanotubes/polyimide nanocomposites for microwave absorption. Compos Part A – Appl Sci Manuf 2012;43(12):2241–8.
[4] Wu Y, Han M, Liu T, Deng L. Studies on the microwave permittivity and electromagnetic wave absorption properties of Fe-based nano-composite flakes in different sizes. J Appl Phys 2015;118:023902.
[5] Feng Y, Qiu T. Preparation, characterization and microwave absorbing properties of FeNi alloy prepared by gas atomization method. J Alloy Compd 2012;513:455–9.
[6] Yang Y, Xu C, Xia Y, Wang T, Li F. Synthesis and microwave absorption properties of FeCo nanoplates. J Alloy Compd 2010;493(1–2):549–52.
[7] Feng Y, Tang C, Qiu T. Effect of ball milling and moderate surface oxidization on the microwave absorption properties of FeSiAl composites. Mater Sci Eng B – Adv 2013;178(16):1005–11.
[8] Lv HL, Ji GB, Wang M, Shang CM, Zhang HQ, Du YW. FeCo/ZnO composites with enhancing microwave absorbing properties: effect of hydrothermal temperature and time. RSC Adv 2014;4(101):57529–33.
[9] Liu XG, Li B, Geng DY, Cui WB, Yang F, Xie ZG, et al. (Fe, Ni)/C nanocapsules for electromagnetic-wave-absorber in the whole Ku-band. Carbon 2009;47(2):470–4.
[10] Yi L, Hu G, Li H. Hierarchical electromagnetic absorption in micro-waveguide stuffed with magnetic media for resin-based composites of graphene nanosheets and manganese oxides. Compos Part A – Appl Sci Manuf 2015;76:233–43.
[11] Yousefi N, Sun X, Lin X, Shen X, Jia J, Zhang B, et al. Highly aligned graphene/polymer nanocomposites with excellent dielectric properties for high-performance electromagnetic interference shielding. Adv Mater 2014;26(31):5480–7.
[12] Chen Z, Xu C, Ma C, Ren W, Cheng HM. Lightweight and flexible graphene foam composites for high-performance electromagnetic interference shielding. Adv Mater 2013;25(9):1296–300.
[13] Chen Y, Zhang H-B, Huang Y, Jiang Y, Zheng W-G, Yu Z-Z. Magnetic and electrically conductive epoxy/graphene/carbonyl iron nanocomposites for efficient electromagnetic interference shielding. Compos Sci Technol 2015;118:178–85.
[14] Chen Y, Lei Z, Wu H, Zhu C, Gao P, Ouyang Q, et al. Electromagnetic absorption properties of graphene/Fe nanocomposites. Mater Res Bull 2013;48(9):3362–6.
[15] Pan G, Zhu J, Ma S, Sun G, Yang X. Enhancing the electromagnetic performance of Co through the phase-controlled synthesis of hexagonal and cubic Co nanocrystals grown on graphene. ACS Appl Mater Interfaces 2013;5(23):12716–24.
[16] Zong M, Huang Y, Zhao Y, Sun X, Qu C, Luo D, et al. Facile preparation, high microwave absorption and microwave absorbing mechanism of RGO-Fe_3O_4 composites. RSC Adv 2013;3(45):23638–48.

[17] Singh VK, Shukla A, Patra MK, Saini L, Jani RK, Vadera SR, et al. Microwave absorbing properties of a thermally reduced graphene oxide/nitrile butadiene rubber composite. Carbon 2012;50(6):2202–8.
[18] Du Y, Liu W, Qiang R, Wang Y, Han X, Ma J, et al. Shell thickness-dependent microwave absorption of core–shell Fe_3O_4@C composites. ACS Appl Mater Interfaces 2014;6(15):12997–3006.
[19] Gong YX, Zhen L, Jiang JT, Xu CY, Shao WZ. Synthesis and microwave electromagnetic properties of CoFe alloy nanoflakes prepared with hydrogen-thermal reduction method. J Appl Phys 2009;106(6):064302.
[20] Liu X, Chen Y, Cui X, Zeng M, Yu R, Wang G-S. Flexible nanocomposites with enhanced microwave absorption properties based on Fe_3O_4/SiO_2 nanorods and polyvinylidene fluoride. J Mater Chem A 2015;3(23):12197–204.
[21] Lim KM, Kim MC, Lee KA, Park CG. Electromagnetic wave absorption properties of amorphous alloy-ferrite-epoxy composites in quasi-microwave band. IEEE Trans Magn 2003;39(3):1836–41.
[22] Liu X, Zhou G, Or SW, Sun Y. Fe/amorphous SnO_2 core–shell structured nanocapsules for microwave absorptive and electrochemical performance. RSC Adv 2014;4(93):51389–94.
[23] Gu Y, Cao Y, Chi H, Liang Q, Zhang Y, Sun Y. Facile synthesis of FeCo/Fe_3O_4 nanocomposite with high wave-absorbing properties. Int J Mol Sci 2013;14(7):14204–13.
[24] Gu S, Duan Y, Duan P, Wang S, Qiu G, Liu Y. Investigation of the absorption properties of the alloys Fe–Ni and Fe–Ni–Cr prepared by mechanical alloying. J Electron Mater 2015;44(7):2331–9.
[25] Liu XG, Ou ZQ, Geng DY, Han Z, Xie ZG, Zhang ZD. Enhanced natural resonance and attenuation properties in superparamagnetic graphite-coated $FeNi_3$ nanocapsules. J Phys D Appl Phys 2009;42:155004.
[26] Wang X, Gong R, Li P, Liu L, Cheng W. Effects of aspect ratio and particle size on the microwave properties of Fe–Cr–Si–Al alloy flakes. Mater Sci Eng A – Struct Mater 2007;466(1–2):178–82.
[27] Lv H, Ji G, Wang M, Shang C, Zhang H, Du Y. FeCo/ZnO composites with enhancing microwave absorbing properties: effect of hydrothermal temperature and time. RSC Adv 2014;4(101):57529–33.
[28] Sun X, He J, Li G, Tang J, Wang T, Guo Y, et al. Laminated magnetic graphene with enhanced electromagnetic wave absorption properties. J Mater Chem C 2013;1(4):765–77.

Please cite this article in press as: Chuai D et al. Enhanced microwave absorption properties of flake-shaped FePCB metallic glass/graphene composites. Composites: Part A (2016), http://dx.doi.org/10.1016/j.compositesa.2016.02.010